




# Understanding the Impact of Fuel on Surfactant Microstructure of Firefighting Foam

Rezawana Islam <sup>\*</sup>, *Materials Science and Engineering, Virginia Tech, 406 Goodwin Hall, 635 Prices Fork Road, Blacksburg, VA 24060, USA*  
Brian Y. Lattimer, *Mechanical Engineering, Virginia Tech, 449 Goodwin Hall, 635 Prices Fork Road, Blacksburg, VA 24060, USA*

**Received:** 12 October 2023/**Accepted:** 11 March 2024

**Abstract.** Aqueous film-forming foam is being phased out due to the environmental impacts of fluorinated surfactants contained in the firefighting foams. To develop an environmentally friendly firefighting foam, it is important to understand the factors controlling the firefighting performance of surfactants. Fuel transport through foam has been considered as a dominant mechanism for foam collapse. Therefore, the impact of fuels (heptane, octane and trimethylbenzene (TMB)) on surfactant microstructure was studied for three different types of surfactants (Capstone, Glucopon, and siloxane) that have applications in firefighting foam. Multiple techniques were used to identify the microstructure and interfacial properties of surfactants with and without exposure to liquid fuel. The ignition time of fuel vapor through foam and solubility of fuel through liquid surfactant solution were measured as well. This work shows fuel solubility has an impact on the surfactant microstructure and interfacial properties. In addition, fuel solubility and vapor pressure affect the ignition time of fuel vapors.

**Keywords:** Fuel concentration measurement, Fuel impact, Interfacial properties, Ignition time, Surfactant microstructure

## 1. Introduction

Aqueous film-forming foams (AFFF) suppress liquid pool fires by spreading over and covering the fuel surface, acting as a physical barrier between fuel vapors and the flame above. AFFF has been in used by fire departments for fire extinguishing, in military, transportation, and fuel storage applications because it is the most effective agent at suppressing large hydrocarbon fuel fires [1–3]. AFFF is a combination of fluorocarbon surfactants, hydrocarbon surfactants, additives and water. It is the most efficient firefighting foam due to fluorocarbon surfactants in its formulations, which can lower the surface tension of the foam solution significantly. Its high effectiveness in fire extinguishment is provided by not only a foam layer but also an

---

\* Correspondence should be addressed to: Rezawana Islam, E-mail: rezawana@vt.edu



aqueous film layer on the surface of liquid fuel upon AFFF application [4]. Fluorinated surfactants in AFFF are bio-persistence and bio-accumulative in nature. Due to this reason, they are being banned internationally. This includes a complete phase-out of AFFF from the U.S. DoD by October 1, 2024. Phase out of AFFF leads to finding an environmentally friendly alternative for current AFFF.

The fire extinguishing mechanism of traditional AFFF is the insulation of liquid fuel from oxygen by a foam layer and aqueous film. During AFFF extinguishing fire, the liquid drained out of the foam can form an aqueous film on the surface of liquid fuel relying on the very low surface tension of the liquid containing fluorocarbon surfactant [4]. The criterion for film formation is based on the spreading coefficient given by Harkins and Feldman [5] as

$$\text{Spreading coefficient (S)} = \sigma_{\text{fuel}} - \sigma_{\text{foam solution}} - \sigma_{\text{interfacial}}$$

$\sigma_{\text{fuel}}$  and  $\sigma_{\text{foam solution}}$  are the surface tensions of the fuel and aqueous surfactant solution respectively and  $\sigma_{\text{interfacial}}$  is the interfacial tension between the fuel and solution. A zero or negative value for the spreading coefficient indicates an inability to form the aqueous film.

Aqueous film formation is considered an important mechanism of foam fire suppression. However, previous research has demonstrated questionable relationships between this mechanism and fire extinguishment performance [6]. Instead of focusing on aqueous film formation and surfactants with very low surface tension, Hinnant et al. [7], showed that the foam layer formed by AFFF is very effective at suppressing fuel vapors formed on a fuel surface. This was shown by measuring fuel vapor concentration above two AFFF covered fuel pools (methylcyclohexane and isooctane) with and without the ability to form the aqueous film. Macroscopic features of the foam such as bubble size and distribution, gas properties (water solubility and diffusivity), surface tension, and solution rheology are important features of foam [8, 9]. The effects of varying the fuel type and temperature beneath the foam were shown to vary spreading coefficient and have demonstrated that forming a film (i.e., positive spreading coefficient) does not correlate to vapor blockage or fire performance [7, 10, 11]. Fuel structure was observed to play a role in fire extinguishment and foam layer degradation with aromatics being more difficult to extinguish compared with alkanes, cyclo-alkanes, and alkenes [12]. Snow et al. [13] revealed that surfactant chemical structure, hydrophilicity hydrophobicity balance affects fire suppression. Fuel transport through the foam was proposed as being a dominant reason for foam collapse, especially with hydrocarbon surfactant where lamellae is more permeable to fuel [7].

The fuel transport mechanism can be divided into four different steps as illustrated in Figure 1: (1) solubility of the fuel into the foam solution, (2) vaporization in the gas bubble, (3) diffusion of fuel in the lamellae, and (4) re-dissolving in the solution around the bubble. Though fuel transport was identified as a potential mechanism that affects foam collapse and extinguishment performance, the parameters controlling these phenomena are unidentified.

It was hypothesized that fuel transport will impact surfactant microstructure. To understand fuel transport, a liquid-liquid setup was developed to study loca-

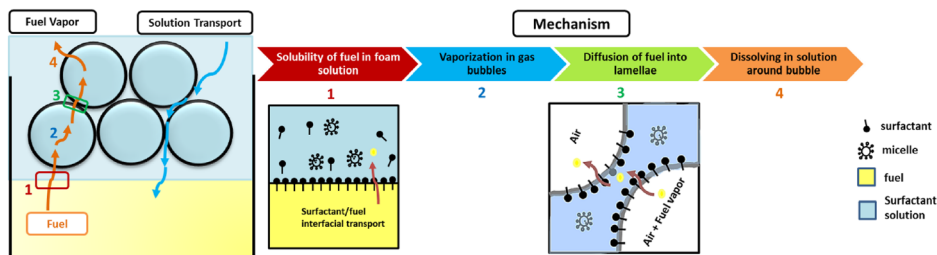


**Figure 1. Fuel transport mechanism through a foam blanket.**

tion 1 from Figure 1, where a layer of fuel was placed at the top of surfactant solution as a second phase. The surfactant solution-fuel interface was used to study interfacial properties and samples were extracted from the surfactant solution side for microstructural study.

To date, the effects of fuel transport into the foam solution as well as surfactant transport out of the foam into the liquid fuel have not been fully quantified or demonstrated. For foam solution in air without the presence of fuel, a variety of advanced experimental methods were used in other applications to quantify and visualize the microscopic changes in surfactants and their effect on the solution transport properties. Surfactants exist on the nanoscale; therefore, cryogenic transmission electron microscopy (cryo-TEM) was used to visualize surfactant structure [14], micelle assembly [15], and changes in microstructure for fluorocarbon–hydrocarbon surfactant mixtures [14]. The micelles ranged from less than 5 nm up to 50 nm with some micelles being spherical while others are more wormlike in structure. Small angle neutron scattering (SANS) was used to quantify micelle assembly structure and surface concentration [16]. Measurements on single lamella or bubbles were used to isolate parameters affecting transport [17, 18]. Numerous studies have demonstrated that cryo-TEM and SANS can be used collectively to characterize the micelle microstructural details of surfactant solutions [14, 19, 20]. However, none of these studies have explored the changes in surfactant solution microstructure after exposure to liquid fuels. In addition, previous literature [7] has reported that hydrocarbon surfactants solubilizes more fuel than fluorocarbon. There is a lack of evidence on the impact of fuel solubility on microstructure in the bulk of firefighting foam.

This study aims to quantify the impact of liquid fuel diffusion on the surfactant solution microstructure. To assess these, three different types of surfactants (fluorocarbon (Capstone 1157), hydrocarbon (Glucopon 600 CS UP), and siloxane (Gelest 6185) into aqueous solution) and two types of fuel (n-alkane (heptane, octane), aromatic (TMB)) were explored. Various experiments were performed to observe micelle size and shape with or without exposure to fuel. Interfacial properties were measured for different surfactant solution/fuel interfaces. The quantity of fuel diffused into surfactant solution was measured. Ignition time was measured for fuel vapor that was transported through the foam. The results from this study will help us understand (1) the detailed microstructure of the Capstone, Glucopon, and siloxane, (2) impact of fuel on their microstructure (3) identify some of the factors affecting the microstructure.

## 2. Experimental Details

### 2.1. Materials

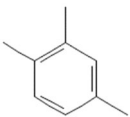
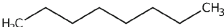

In this study, our goal was to investigate the single surfactants (fluorosurfactant Capstone and hydrocarbon surfactant Glucocon) used in Ref-AFFF to evaluate the factors affecting fuel transport. Siloxane surfactant has been explored as a potential alternative to fluorosurfactant in firefighting foam formulation. In addition, Capstone, Glucocon, and siloxane were chosen as firefighting foam surfactants due to their greater ability to reduce surface tension. Gasoline was used as the fuel in a pool for fire extinction test in MilSpec standard, the most rigorous method for evaluating firefighting foam performance. However, the presence of TMB in gasoline makes it harder to extinguish [12]. Most other test protocols use heptane as fuel for fire extinction tests [12]. In this work, primarily we have studied TMB and heptane to understand the difference in fuel impact on surfactant microstructure. In addition, have studied octane from n-alkane category to observe the ignition time. TMB, heptane, and octane have a constant composition, unlike gasoline. These fuels represent two different categories of fuel: n-alkane (heptane, octane), and aromatic (TMB). Due to the higher flash point, it was challenging to ignite TMB at room temperature. Therefore, a two components (25% trimethylbenzene + 75% heptane) simulant for gasoline were used for evaluating ignition time in the presence of an aromatic component (TMB) since suppression time for this mixture of fuel is very close to the suppression time for gasoline [12].

*2.1.1. Fuel* The physical properties of TMB, heptane, and octane is presented in Table 1. All the physical properties are taken from the Safety data sheet for these fuels [21–23]. The calculated vapor pressure of 25%TMB-75%heptane is 37.9 mm Hg.

*2.1.2. Surfactant* Three different types of surfactants Capstone 1157, Glucocon 600 CS UP, and Gelest 6185 were used for this study with properties given in Table 2 and structures provided in Fig. 2. Various experiments were done on surfactant solutions and characterized at a range of surfactant concentrations to determine interfacial properties. Ignition tests, fuel concentration measurements, Dynamic light scattering (DLS) have been done at 5 times the Critical micelle concentration (CMC) based on surfactant concentration, which is approximately the surfactant concentration used in Reference AFFF [24]. Cryo-TEM, SANS were done at 7 times higher than Capstone and 10 times higher than Glucocon surfactant concentration consecutively.

*2.1.3. Sample Preparation* Figure 3 shows the sample extraction setup. The transport of fuel into the surfactant solution was quantified through a diffusion experiment with ~ 15 ml liquid fuel over a layer of ~ 15 ml surfactant solution. The fuel and surfactant solution two-phase system were prepared in a 20 ml glass vial. After pouring the surfactant solution in the glass vial, a syringe was inserted and then a fuel layer was added at the top of the surfactant solution to avoid any contamination on the needle while extracting the sample using the syringe. Before extracting the sample, waited 15 min for the fuel and surfactant solution to reach equilibrium at room temperature, this will allow diffusion processes to equilibrate before measuring. The surfactant solution sample was extracted from 10 mm away from the

**Table 1**  
**Physical Properties of Fuel**

Fuel	Chemical formula	Structure	Water solubility (mg/L)	Vapor pressure (mmHg)	Flash point (°C)
1,2,4 Tri-methylbenzene	C <sub>9</sub> H <sub>12</sub>		57	1.72	48
Octane	C <sub>8</sub> H <sub>18</sub>		0.66	14	13
Heotane	C <sub>7</sub> H <sub>16</sub>		3.4	48	- 4

**Table 2**  
**Surfactant Properties**

Name	Molecular weight (g/mol)	Molecular length (Å)	Tail length	Tail type	Head type
Capstone 1157	570	19.322	Long	Fluorocarbon	Zwitterionic
Glucopon 600 CS UP	386	18.779	Long	Hydrocarbon	Nonionic
Gelgest 6185	550	39.945	Branched	Siloxane	Nonionic

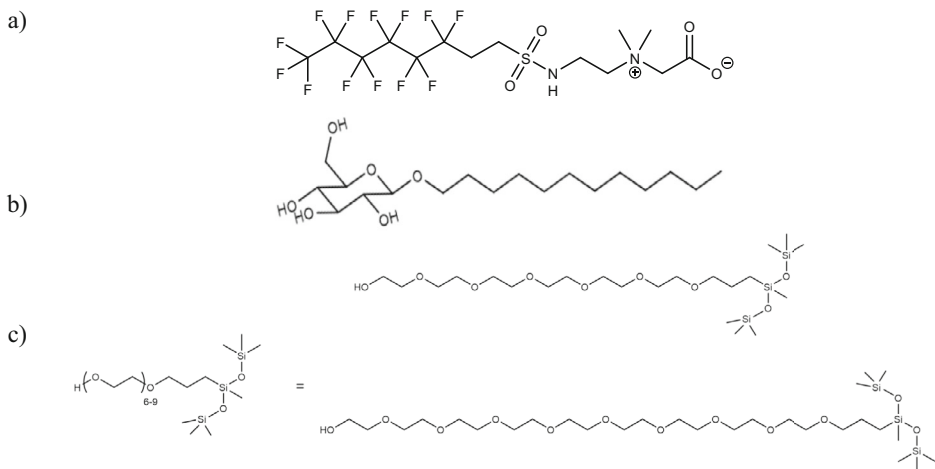


**Figure 2. Surfactant structures (a) Capstone 1157 (b) Glucopon 600 CS UP (c) Gelgest 6185.**

interface. The extracted sample (referred to as two-layer interaction sample in this document) was used for microstructural and fuel concentration measurements.

## 2.2. Methods

Small angle neutron scattering (SANS), Cryogenic transmission electron microscopy (Cryo-TEM), and Dynamic light scattering (DLS) were used to measure the surfactant microstructure in the bulk of the surfactant solution with or without exposure to fuel. A Tensiometer was used to measure the interfacial properties (surface tension (SFT), interfacial tension (IFT), critical micelle concentration (CMC), surface excess, etc.). The concentration of fuel in the surfactant solution quantified using UV/Vis spectroscopy. An ignition test was conducted to quantify the ignition time of fuel vapors transported through a layer of foam. For ignition tests foams were prepared using a Dynamic Foam Analyzer (DFA100).

*2.2.1. Cryogenic Transmission Electron Microscopy (Cryo-TEM)* As shown in Figure 3 the samples were extracted and vitrified to visualize the micelle structure. Vitrification was done in a controlled environment vitrification system (CEVS) and plunged into liquid nitrogen at its freezing point using a lacey carbon grid. The vitrified specimens were stored under liquid nitrogen ( $-196^{\circ}\text{C}$ ). Then samples were observed in a ThermoFisher titan krios g4 with a direct electron detector (falcon 3EC). Cryo-TEM measurements were conducted at the CNMS facility of the Oak Ridge National Laboratory, Oak Ridge, TN.

*2.2.2. Small Angle Neutron Scattering (SANS)* To observe the micelle size and shape in the bulk, a liquid–liquid interface was created by placing a fuel layer at the top of the surfactant solution as described in Figure 3. Two different locations away from the interface, one on the fuel side (top phase) and the liquid side (bottom phase) were chosen to study. Samples were prepared by dissolving precise quantities of surfactant in  $\text{D}_2\text{O}$  with stirring. Measurements were performed at  $25^{\circ}\text{C}$  in 1 mm path length and quartz Hellma cells. Then raw scattering intensity profile  $I(q)$  versus  $q$  was captured. The intensity profile is a function of the scattering vector,  $q$ . The wavelength ( $\lambda$ ) of the incident neutrons is  $2.5 \text{ \AA}$ . Scattering was performed with the detector positioned separately at 3 and then 4 m from the sample environment, providing a  $q$ -range of approximately  $0.004\text{--}1.4 \text{ \AA}^{-1}$ . SANS measurements were conducted at beamline-6 of SNS facility, Oak Ridge National Laboratory, Oak Ridge, TN.

*2.2.3. Dynamic Light Scattering (DLS)* DLS was performed to observe the micelle size in the bulk using a Malvern Zetasizer Nano ZS. The extracted sample (as shown in Figure 3) was placed in a Polystyrene cuvette at  $25^{\circ}\text{C}$ . Data processing was carried out with a computer attached to the instrument. The average size distribution of the surfactant micelle was recorded. The measurements were repeated three times to check their reproducibility.

*2.2.4. Tensiometer* Surface tension was measured at room temperature using a KRÜSS K100C tensiometer using the Wilhelmy plate method. Each measurement

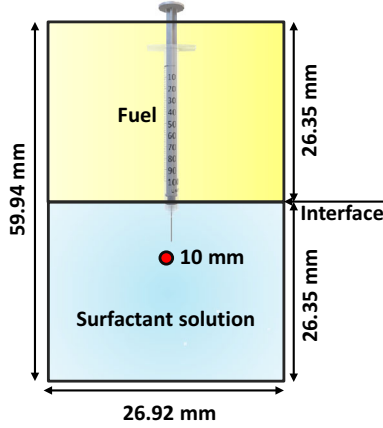


**Figure 3. Experimental setup.**

was an average of five surface tension measurements. Using the automatic dosing unit of the instrument, surface tension was measured at different surfactant concentrations. A plot of surface tension versus surfactant concentration was used to quantify the CMC, which is the lowest concentration where the surface tension does not change when there is an increase in surfactant concentration. Surface tension is linearly dependent on the logarithm of the concentration over a large range. The CMC results from the intersection between the regression straight line of the linearly dependent region and the straight line passing through the plateau. The data was also used to quantify the surface excess. Surface excess is the area-related concentration of surfactant at the surface or interface. The concentration of surfactant at the surface is significantly higher compared to its concentration in the bulk phase. Surface excess has the unit of  $\text{mol}/\text{m}^2$  and is calculated based on the slope of the surface tension data at concentrations below the CMC using the Gibbs equation [25].

$$\Gamma = -\frac{1}{nRT} \cdot \frac{d\gamma}{d\ln(c)} \quad (1)$$

where  $n = 1$  for non-ionic surfactants, neutral molecules, or ionic surfactants,  $\Gamma$  is the equilibrium surface excess ( $\text{mol}/\text{m}^2$ ),  $R$  is the gas constant ( $8.314 \text{ J}/\text{mol}\cdot\text{K}$ ),  $T$  is temperature (K),  $c$  is the bulk surfactant concentration (M),  $\gamma$  is surface tension ( $\text{mN}/\text{m}$ ), and  $d\gamma/d\ln(c)$  is the slope of the surface tension and natural log of surfactant concentration. This was then used to calculate the area per molecule ( $\text{nm}^2$ )

$$A = -\frac{10^{18}}{N_A \Gamma} \quad (2)$$

where  $N_A$  is Avagadro's number ( $6.022 \cdot 10^{23}$  molecules/mol). These measurements were conducted for all surfactants at an air interface and for select surfactants at the solution-fuel interface.

**2.2.5. UV–Vis Spectroscopy** UV–Vis measurements were done to quantify the fuel concentration in the bulk using a Hitachi U4100 UV–Vis–NIR spectroscopy. In this work, we measured the TMB water solubility using UV–Vis spectroscopy as a verification of this method. In Figure 4a, the absorbance spectra for known concentrations of TMB in water were measured to prepare the standard curve in Figure 4b. TMB was added to surfactant solution in known concentrations of 0.4, 0.8, 1.2, 1.6, and 2 wt%. A stirring plate and a magnetic stirring bar were used for approximately 10 min for mixing. Afterwards, waited for 15 min for sample equilibration and transferred it to the cuvette for analysis [26]. The absorption peak from 300 to 230 nm was used for the analysis of TMB. The absorbances of all the standard samples were recorded keeping water as the baseline presented in Figure 4a.

For TMB-water analysis, a sample was extracted from a two-layer interaction sample of water (bottom phase) and TMB (top phase) as shown in Figure 3. The absorbance attained placed into the standard curve (absorbance versus Fuel concentrations Figure 4b) to quantify the concentration of TMB in water. The value was 0.006 wt% which is close to the reported value of 57 mg/l or 0.0057 wt.% in water [21].

**2.2.6. Dynamic Foam Analyzer (DFA)** The Dynamic Foam Analyzer (DFA100–KRÜSS) was used to quantify the foam quality on a bench scale. We intended to use a consistent way to generate foam. DFA is such a method that can produce foam in a consistent and reliable way and provide all the foam properties for various surfactants studied in the laboratory. In this method, a surfactant solution (35 mL) was introduced into the DFA glass cylinder container, which has a porous disk with a pore size ranging from 16 m to 40 m at the bottom of the cylinder. Air then flows through the sparger at a rate of 0.2 L/min for 40 s. The expansion ratio of each surfactant is calculated by measuring the foam volume using a line sensor after 40 s of air addition. After foam generation, the initial bubble diameter, initial bubble distribution, liquid drainage from the foam, and expansion ratio are studied for each of the foams generated. The bubble sizes were directly obtained from ADVANCE software.

**2.2.7. Ignition Test** An ignition test was developed (Figure 5) to quantify the ignition time of fuel vapors transported through a layer of foam. The test was developed with inspiration from the open-cup flashpoint test that is commonly used to assess the flammability of fuels. For the ignition test, a 75 mm diameter, 25 mm deep glass dish was filled with a 15 mm thick layer of foam, then 25 mL of fuel was injected with a syringe through the foam so that the foam height was close to the top of the dish. After the fuel was injected through the foam, a pilot flame igniter was positioned over the top of the foam in the center of the pan. The changes in foam during the experiment were captured using a high-resolution video camera.

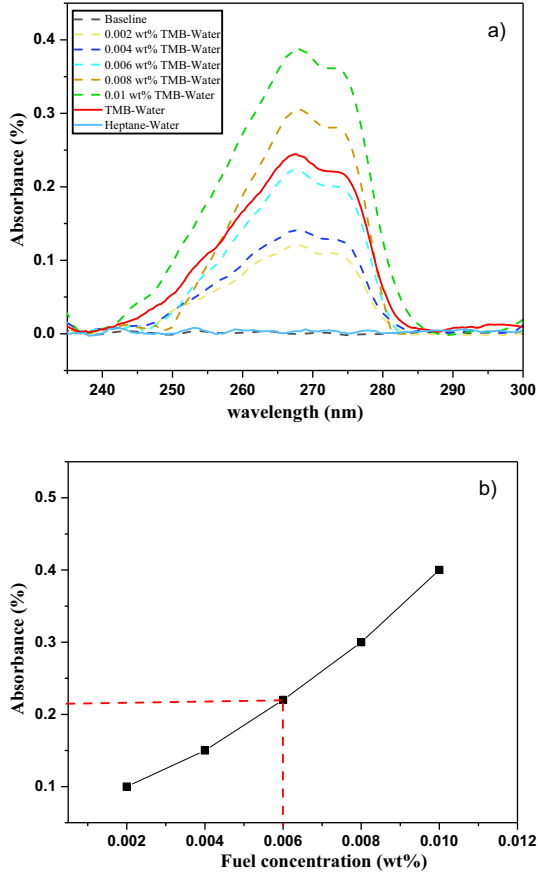


**Figure 4. UV-Vis spectra (a) absorbance versus wavelength (b) standard graph.**

### 3. Results

#### 3.1. Packing Parameter

Surfactants tend to self-assemble themselves into micelle above their critical micelle concentration (CMC). The molecular packing parameter ( $p$ ), a theory developed by Israelachvili et al. to describe or calculate the shape of molecular self-assembled structures in a surfactant solution [27].  $p$  can be estimated using the following equation:

$$p = \frac{v}{a_0 l} \quad (3)$$

where,  $v$  and  $l$  are the volume ( $\text{nm}^3$ ) and length (nm) of the hydrophobic tail,  $a_0$  = the effective head group area ( $\text{nm}^2$ ) at the interface of the hydrophobic core-hydrophilic media.

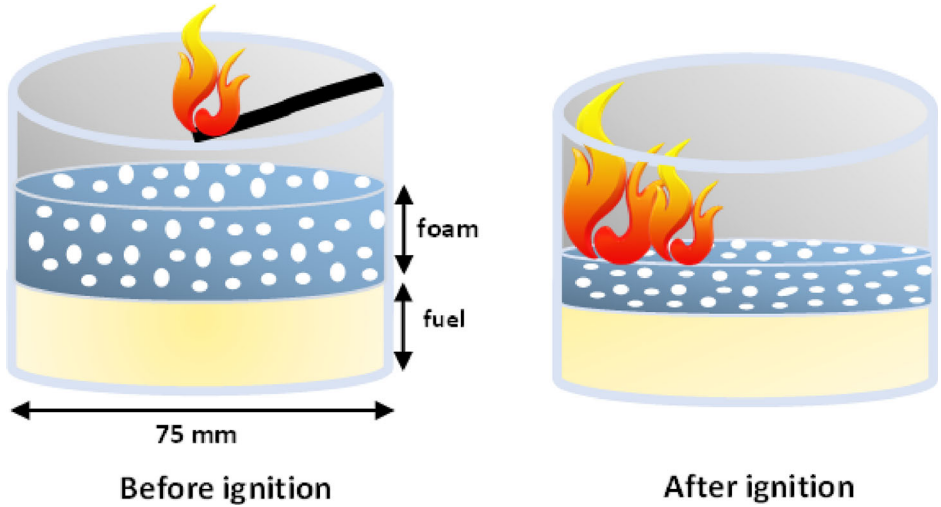


**Figure 5. Ignition test set up.**

This parameter allows a simple and intuitive insight into the relationship between molecular structures and the shape of self-assembly. For example,  $0 < p \leq 1/3$  is for spherical micelles,  $1/3 < p \leq 1/2$  is for cylindrical ones,  $1/2 < p \leq 1$  is for bilayer structures, such as vesicles, and  $p > 1$  is for inverted structures [28–30].

The chemical structures of surfactants used in this study were drawn using Chem sketch. Tail length and volume for the surfactant structures were attained using the Avogadro software [31]. Effective head group area was calculated from tensiometer discussed in the Interfacial properties section of this paper. The calculated  $p$  values indicated the shape of the micelles formed (i.e., vesicles, worm-like and inverted structure for Capstone, Glucopon and siloxane surfactants respectively) [30]. See supporting information (Table S1) for more details (see Table 3).

### 3.2. Microstructural Features of Surfactants

**3.2.1. Cryogenic Transmission Electron Microscopy (Cryo-TEM)** **3.2.1.1. Capstone** The self-assembly behavior of Capstone with or without exposure to liquid TMB was observed by cryo-TEM. As shown in Figure 6a, it was noticeable that Capstone molecules self-assemble into vesicles in solution rather than forming micelles consistent with literature [32]. At a concentration higher than CMC (7 times higher than CMC based on surfactant concentration), observed single lamellar vesicles formed by Capstone molecules, and the diameters of vesicles are  $\sim 37$  nm. In Capstone-TMB (Figure 6b), the size of vesicles increased and diameter is around 194 nm. In some cases, they formed multilamellar vesicles can be observed clearly in Figure 6b. Cryo-TEM images showed the impact of Trimethylbenzene (TMB) on the Capstone vesicle and revealed that adding TMB results in two changes (1) an increase in aggregation/grouping of the vesicles and (2) an increase in the diameter and (sometimes) membrane layers. Most likely Capstone

**Table 3**  
**Calculated p Value and Graphical Representation of Self-Assembly Structure**

	Surfactant	$p = \frac{v}{a_0 l}$	Structure formed	
	Capstone	$> 1/2$	Vesicles	
	Glucopon	$1/2$	Worm-like	
	Siloxane	$> 1$	Inverted structure	

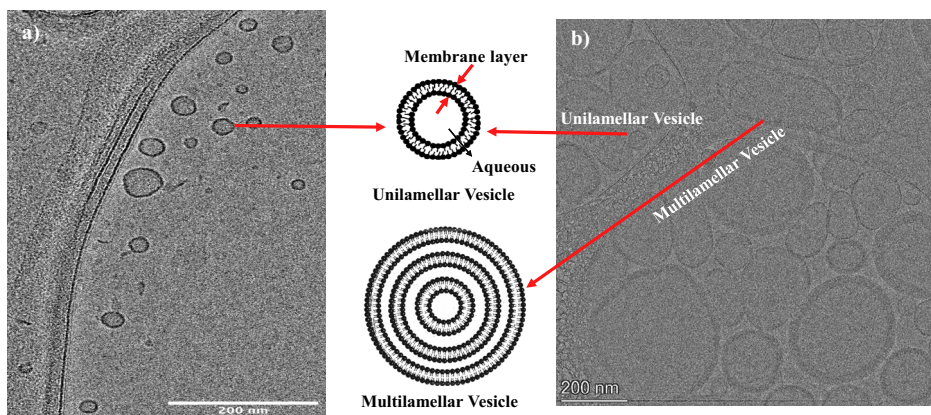


**Figure 6. Cryo-TEM for (a) Capstone (b) Capstone-TMB.**

was solubilizing TMB and forming swollen micelle but the location of fuel molecules was not confirmed for Capstone-TMB from this analysis.

3.2.1.2. *Glucopon* Cryo-TEM reveals self assembly behavior of Glucopon 600 CS UP in aqueous solution. Glucopon formed worm like micelles as shown in Figure 7, at a concentration higher than CMC (10 times higher than CMC based on surfactant concentration). We observed worm like micelle for Glucopon-TMB presented in Figure 7. Visually from cryo-TEM no difference was observed in terms of micelle size and shape between Glucopon and Glucopon-TMB.

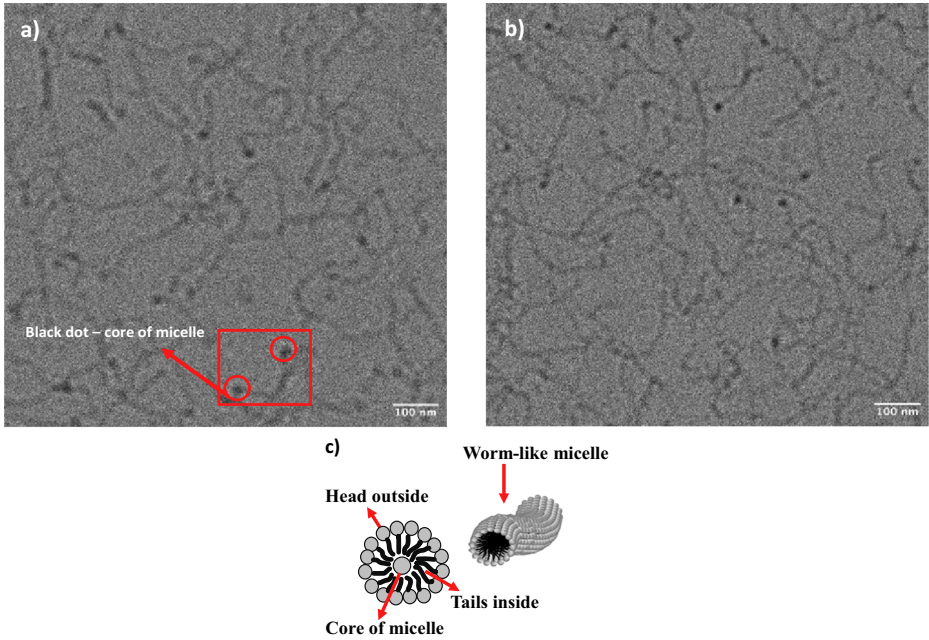


**Figure 7. Cryo-TEM for (a) Glucopon (b) Glucopon-TMB (c) illustration of worm-like micelle.**

**Table 4  
SANS Measurement for Capstone**

Sample	Thickness (Å)	d_spacing (Å)
Capstone	28 ± 0.2	325 ± 9.08
Capstone-heptane	27 ± 0.19	331 ± 6.92
Capstone-TMB	28 ± 0.22	373 ± 8.92

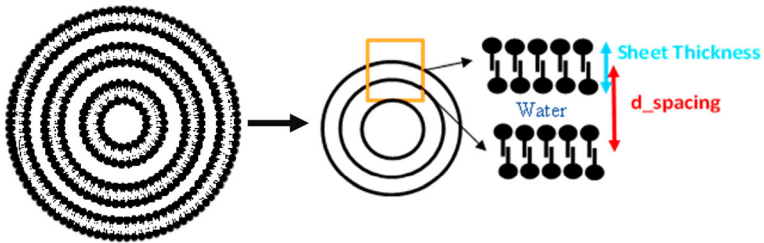


**Figure 8. a Multilamellar vesicle b d\_spacing for vesicles.**

**Table 5**  
**SANS Measurement for Glucopon**

Sample	Radius (Å)	Length (Å)
Glucopon	14.78 ± 0.11	654 ± 14
Glucopon-heptane	14.81 ± 0.07	633 ± 13
Glucopon-TMB	14.66 ± 0.08	728 ± 16

3.2.2. *SANS* For in-situ observation of structures in the bulk and fuel phase, measurements were performed using SANS. Scattering profiles are included in the supporting information section.

3.2.2.1. *Capstone* The scattering profile (see Figure S1 for supporting information) indicated that Capstone 1157 formed a lamellar structure. The form factor “lamellar structure paracrystal” was the representation of large multilamellar vesicles. Sheet thickness ( $t$ ) was  $\sim 28$  Å and similar for Capstone, Capstone-heptane, and Capstone-TMB. However, the  $d_{\text{spacing}}$  occurred to increase for the Capstone-TMB (Table 4). It was confirmed from the Cryo-TEM images that the presence of TMB increased the vesicle size and membrane layers (Figure 6). Therefore, it was likely that the  $d_{\text{spacing}}$  would increase (Figure 8). The  $d_{\text{spacing}}$  (Table 4) was similar for Capstone and Capstone-heptane indicating that heptane did not impact the vesicle size.

3.2.2.2. *Glucopon* The scattering profile (see Figure S2 for supporting information) from SANS result showed that Glucopon formed worm like micelle. The form factor “flexible cylinder elliptical” was a representation of a worm-like micelle. The radius was  $\sim 14$  Å for Glucopon. The overall length of the micelle was  $654 \pm 14$  Å (Table 5). In the two-layer sample, length of the micelles in the bulk of the solution was somewhat decreased due to presence of heptane in the top phase. In this case, more surfactants were traveling to the interface, thereby decreasing the micelle length. For the case of TMB on the top phase, micelles were increasing in length by 100 Å (Table 5). The characteristic of worm-like micelles is that they grow in length to accommodate fuel molecules [33]. As a result, the increasing length of the worm like micelle indicated fuel solubilization.

3.2.2.3. *Siloxane* According to SANS fitted model (see Figure S3 from supporting information), siloxane surfactant was ellipsoidal. In the presence of heptane and TMB on the top phase (Table 6), micelles in the bulk of the solution did not change shape and radius. Therefore, TMB and heptane did not affect the microstructure of the siloxane surfactant. However, the scattering data (see Figure S4 from supporting information) indicated the presence of structures in the heptane phase (top phase in Figure 3) for Siloxane-heptane. This confirmed the formation of reverse micelle. SANS data was fitted using sphere model and radius was around  $363 \text{ \AA}$  (Table 7).

**Table 6**  
**Radius for Siloxane from SANS (Bottom Phase)**

No	Name	Radius (Å)
1	Siloxane	20 ± 0.03
2	Siloxane-heptane	20 ± 0.03
3	Siloxane-TMB	20 ± 0.04

**Table 7**  
**Radius for Siloxane from SANS (Top Phase)**

Name	Model	Radius (Å)
Siloxane-heptane	Sphere	363 ± 11

3.2.3. *DLS* Dynamic light scattering (DLS) measurements were performed to assess the change of micelle size in the bulk of the surfactant solution due to fuel exposure. For different surfactant micelles with fuel exposure resulted in increase size and sometimes two different size distributions were observed, see Figure 9. TMB showed much higher effect in the microstructure compared to heptane for both Capstone and Glucopon. The polydispersity for the reported sizes was around 0.2–0.3 which means a moderately polydisperse distribution type.

### 3.3. Interfacial Properties

To observe the impact of fuel at the interface surface tension, interfacial tension, and surface excess, CMC has been measured with or without the presence of fuel.

3.3.1. *Surface Tension* Surface tension results were presented in Figure 10 for all three surfactants at initial concentrations higher than their CMC. This includes both the surface tension (SFT) for air/surfactant solution as well as interfacial surface tension (IFT) for fuel/surfactant solution. Comparing the SFT for three single surfactants, Capstone has its greatest ability to lower the surface tension at the air/surfactant solution interface (15.99 mN/m) while Glucopon has the highest (28.45 mN/m). All values were consistent with those reported elsewhere [34, 35].

The results in Figure 10 demonstrated that IFT value is fuel and surfactant type dependent. Glucopon-TMB IFT value of 11.57 mN/m is higher than Glucopon-heptane IFT value of 5.51 mN/m. In most cases, IFT values are in the range of 4–12 mN/m except for Siloxane-heptane which has a very low IFT of 0.7 mN/m. This indicated that the siloxane surfactant made the heptane and aqueous solution more miscible.

3.3.2. *CMC* The CMC for the solutions was determined using surface tension data at different surfactant concentrations. Below the CMC, the surface tension

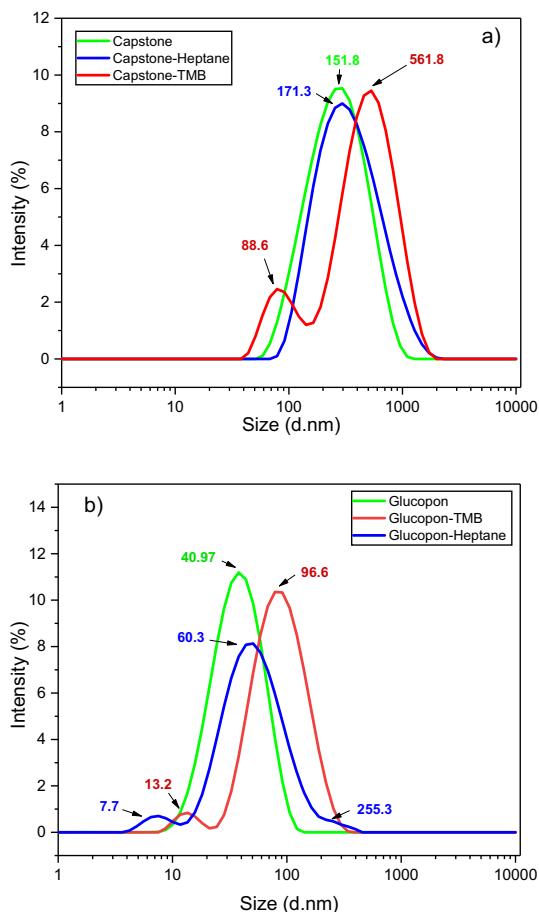


**Figure 9. DLS results (a) Capstone (b) Glucopon with and without fuel exposure.**

increases with a decrease in surfactant level while above the CMC the surface tension is constant. The surfactant concentration at the intersection of these two lines is the CMC. The CMC value measured for Capstone, Glucopon, and Siloxane surfactant solutions of 0.011, 0.012, and 0.009 wt.% of surfactant, respectively (Figure 11). CMC values were consistent with literature for all the cases [34, 35].

**3.3.3. Impact of Fuel on CMC** CMC values for Capstone, Capstone-heptane, and Capstone-TMB are 0.011, 0.011, and 0.006 wt.% respectively (Figure 12a). A similar trend was observed for CMC values for Glucopon, Glucopon-heptane, and Glucopon-TMB which are 0.012, 0.012, and 0.006 wt.% respectively (Figure 12b). Results showed that for both Capstone and Glucopon surfactants, CMC with heptane-surfactant solution was same as air-solution. However, CMC with TMB-surfactant solution was lower than air-solution. This indicated that the TMB

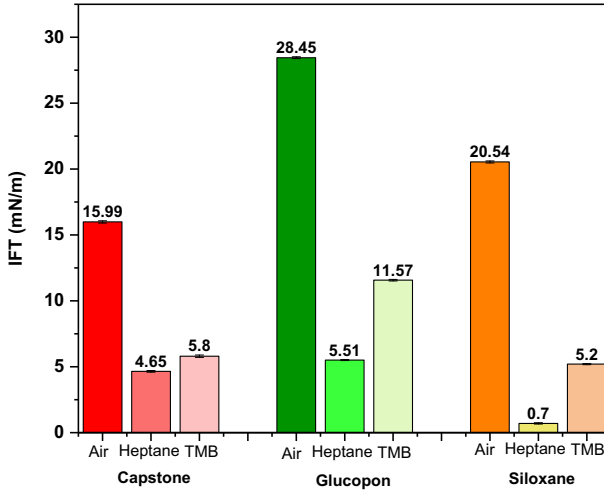


**Figure 10. Surface tension (SFT) and Interfacial tension (IFT) values.**

interacted with the surfactant solution causing micelle formation at lower concentrations. Hence, decreasing CMC in the presence of TMB.

CMC values for Siloxane, Siloxane-heptane, and Siloxane-TMB are 0.009, 0.06, and 0.009 wt.% respectively (Figure 12c). CMC with TMB-surfactant solution was same as air-solution. However, CMC with heptane-solution was higher than air-solution. This indicated that near CMC region, surfactants travel to the fuel phase rather than forming micelle in the bulk of surfactant solution. Hence, CMC value increased. This indicated the formation of reverse micelle.

**3.3.4. Surface Excess** Figure 13 showed that surface excess for Capstone-TMB in comparison to Capstone was decreased to 70%, for Glucopton-TMB in comparison to Glucopton decreased to 52%. These results indicated that TMB caused surfactants to go away from the interface and reduced surface excess. For heptane-siloxane in comparison to siloxane surface excess was reduced to 73%, meaning that heptane caused siloxane surfactants to move away from the interface reducing the surface excess. A similar trend for low surface excess was observed for Trisiloxane surfactants in the presence of hydrocarbon fuels [36].

### 3.4. Impact of Surfactants on Fuel Solubility

UV-Vis spectroscopy measurements were performed to quantify the fuel solubility in the bulk of the surfactant solution. According to previous literature octane, heptane, TMB have 0.000066, 0.0003, and 0.0057 wt.% solubility in water consecutively [21–23] presented in Table 8. Benzene ring fuel (TMB) has higher water solubility than alkane type fuels.

The UV-Vis spectroscopy results revealed that none of the surfactants used in this study increased the solubility of alkane type of fuel (octane, heptane). The absorbance versus wavelength spectrum for Capstone-octane and Capstone-hep-

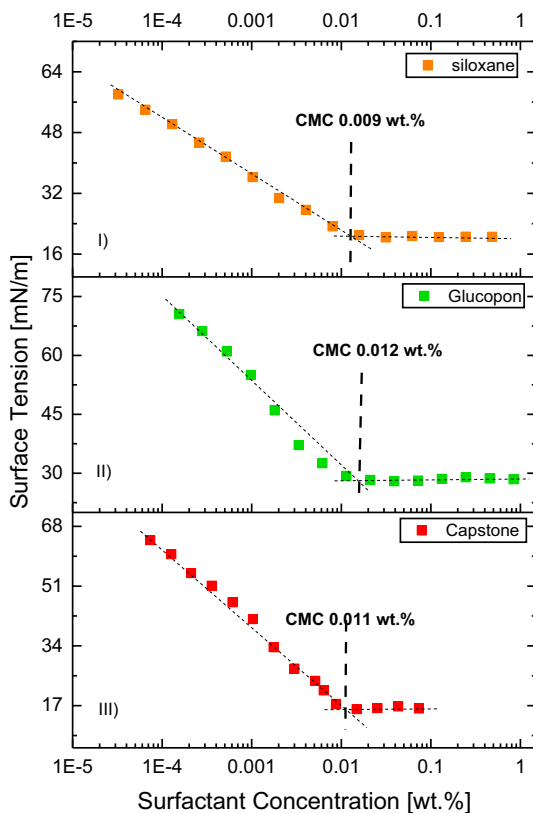


**Figure 11. CMC for surfactants (i) Siloxane (ii) Glucopon (iii) Capstone.**

tane was close to Capstone-baseline (Figure 14a). For Glucopon-octane and Glucopon-heptane was close to Glucopon-baseline (Figure 14b). Therefore, Capstone and Glucopon did not increase the solubility of octane and heptane in water. According to Figure 14a, b Capstone-TMB and Glucopon-TMB absorbance versus wavelength peaks were higher than Capstone-baseline and Glucopon-baseline respectively. Therefore, Capstone and Glucopon surfactant increased the solubility of TMB in water. The concentration of TMB in Capstone and Glucopon solution was found 0.12 wt.% and 0.18 wt.% respectively (Figure 15). According to Figure 14 siloxane did not increase the solubility of octane, heptane, 25%TMB-heptane. The absorbance for siloxane-TMB was slightly higher than siloxane baseline. However, the solubility of TMB in siloxane solution was 0.0038 wt.% smaller than the solubility of TMB in water.

UV-Vis spectroscopy could not detect the solubility of 25%TMB-75%heptane in water. Figure 16 showed that absorbance peak was higher for Glucopon-25% TMB-75%heptane than Glucopon-baseline. Therefore, 25%TMB-75%heptane has solubility in Glucopon solution. For Capstone-25%TMB-75%heptane the absor-

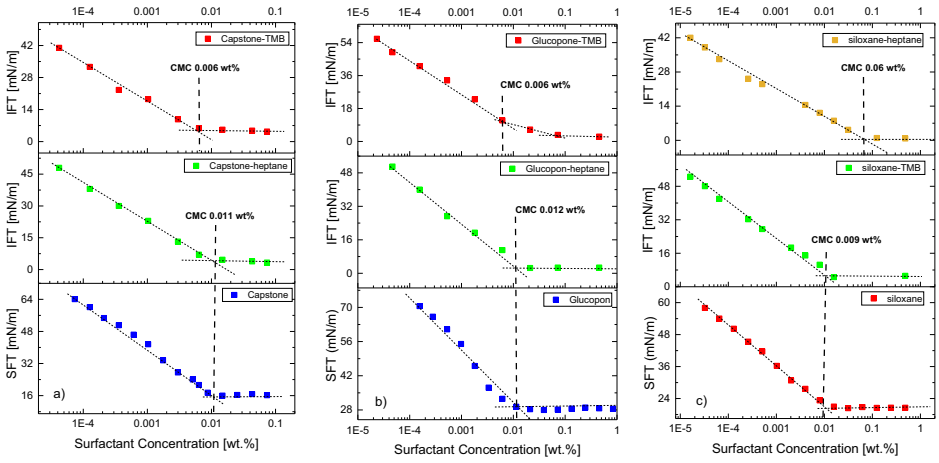


**Figure 12. CMC in the presence of fuel (a) Capstone (b) Glucopon (c) Siloxane.**

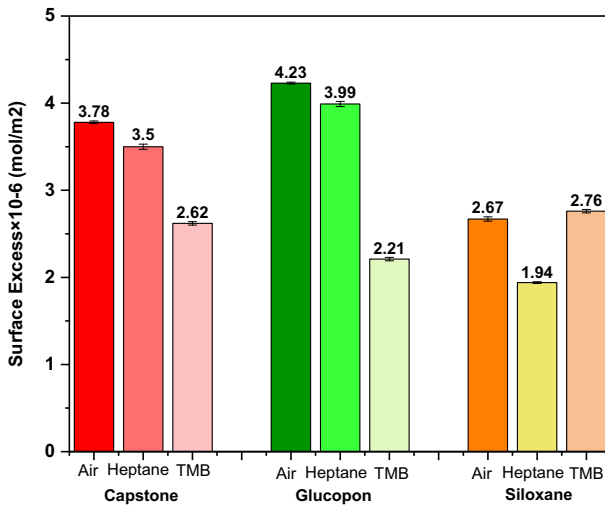


**Figure 13. Surface excess with or without fuel exposure.**

**Table 8  
Water Solubility of Fuel**

Fuel	Water solubility (wt.%)
Octane	0.000066
Heptane	0.00034
TMB	0.0057

*Understanding the Impact of Fuel on Surfactant Microstructure*

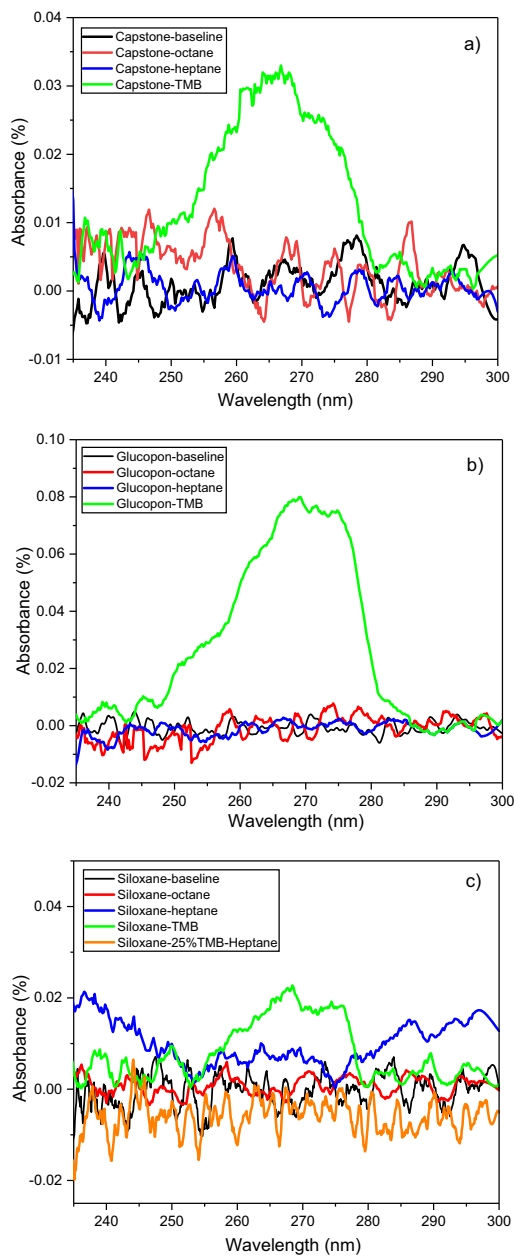


**Figure 14. Solubility of fuel into surfactant solution (a) Capstone (b) Glucopon (c) Siloxane.**

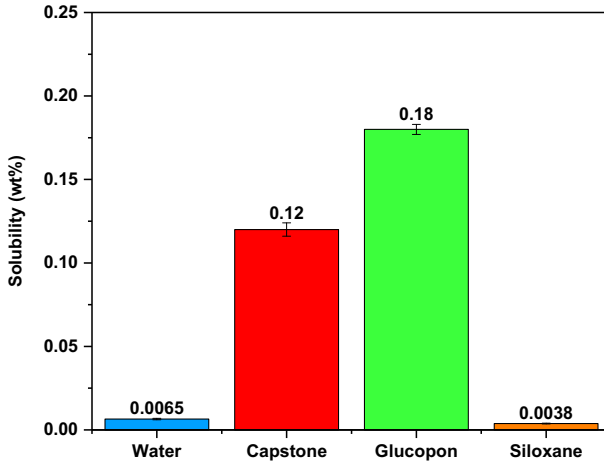


**Figure 15. Solubility of TMB Capstone, Glucopon, and siloxane.**

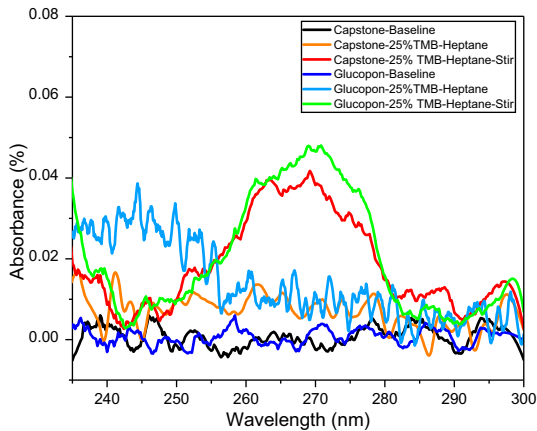


**Figure 16. Solubility of 25% TMB-heptane in Capstone and Glucopon surfactant solution with and without stirring.**

bance peak was close to Capstone-baseline. Therefore, 25%TMB-75%heptane was not soluble in Capstone solution in a static liquid–liquid setup. In the liquid–liquid set up stirring was introduced at the bottom phase (as shown in Figure 3) for 15 min for Capstone-25% TMB-75%heptane before sample extraction. After stirring Capstone-25%TMB-75%heptane showed an absorbance peak higher than Capstone-baseline. Therefore, 25%TMB-75%heptane has solubility in capstone solution with stirring. However, with and without stirring Glucopon-25%TMB-75%heptane showed higher absorbance peaks compared to Capstone-25%TMB-75%heptane. Therefore, 25%TMB-75%heptane has higher solubility in Glucopon solution compared to Capstone solution.

**Table 9**  
**Foam Properties**

Surfactant	Expansion ratio (ER)	25% liquid drainage [s]
Capstone	$7.4 \pm 0.3$	$54.1 \pm 2$
Glucopon	$6 \pm 0.07$	$43.3 \pm 1.3$
Siloxane	$10.5 \pm 0.1$	$65.6 \pm 0.5$

### 3.5. Ignition Test

For ignition tests, foam was generated using DFA as detailed in the experimental section. Three different types of foams and two different types of fuels were used for analysis. Foam properties were observed as well. Ignition time for each type of fuel through different surfactant foam solutions was recorded for analysis purposes.

*3.5.1. Foam Tests* Table 9 highlighted that the expansion ratio for Glucopon was lowest in comparison to Capstone and siloxane. 25% liquid drainage time is lowest for Glucopon. Wetter foam usually drains faster compared to drier foam. Longer drain time has been observed for Capstone due to having smaller bubble diameter compared to Glucopon. Since the mean free paths length would then become higher due to smaller bubble diameter and the solution would have a longer distance to go. However, Siloxane formed comparatively a less wet foam indicated by high expansion ratio compared to Capstone and Glucopon; therefore, a longest drain time [37]. Figure 17 depicts the bubble diameter for three surfactants. Siloxane has the largest and Capstone has the smallest diameter bubble. The decrease in bubble size was most likely due to a decrease in expansion ratio [38]. The bubble size and expansion ratio were dependent on each other but are not dependent on surfactant molecular structure or surface tension [34].

*3.5.2. Ignition Time of Fuel* The ignition time for heptane, octane, and 25%TMB-75%heptane through Capstone, Glucopon, and siloxane foam solution were presented in Figure 18. 25% TMB-heptane has the lowest and Octane has the highest ignition time for all three-surfactant foam solutions tested. Irrespective of the fuel types, Capstone foam solution has the highest, and siloxane foam solution has the lowest ignition time.

## 4. Discussion

The findings from this study show that TMB has affected the microstructure of Capstone and Glucopon due to their higher solubility in surfactant solution. On the other hand, microstructure is unaffected by heptane due to its poor solubility in surfactant solution. The ignition time for fuel mixture 25%TMB-75%heptane is

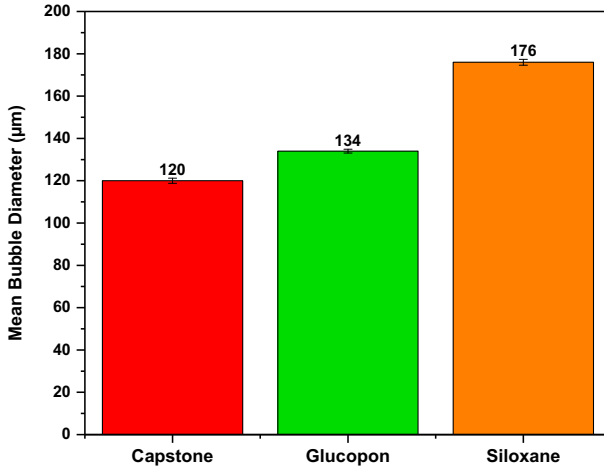


**Figure 17. Bubble diameter.**

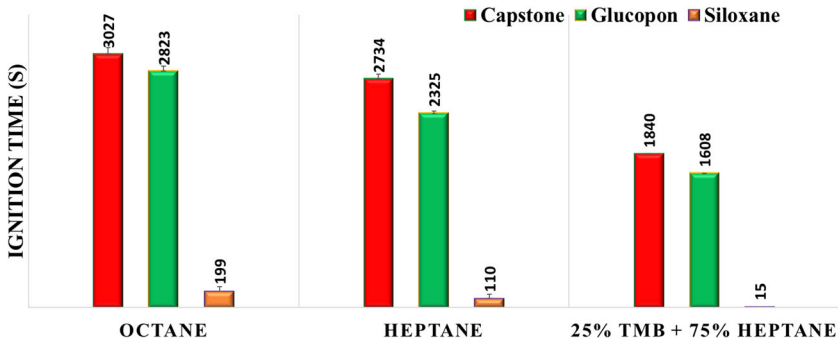


**Figure 18. Ignition test results.**

shorter compared to heptane and octane due to higher solubility in Capstone and Glucopon foam solution.

The solubility of fuel (i.e., the maximum amount of fuel solubilized in surfactant solution) in surfactant solution will have a significant impact on the microstructure. According to SANS and DLS results, heptane did not change the micelle size in the bulk for the three surfactants used in this study significantly. Heptane has 0.0003 wt.% solubility in water which makes them almost insoluble. Fuel concentration measurements (Figure 14) reveal that in a static liquid–liquid setup (Figure 3) Capstone, Glucopon, and siloxane did not increase the solubility of heptane in water. Therefore, due to the poor solubility of heptane in surfactant solutions, no changes in the micelle size or shape have been observed for Capstone, Glucopon, and siloxane. Cryo-TEM, SANS, and DLS reveal that TMB has changed the micelle size for both Capstone and Glucopon.

## *Understanding the Impact of Fuel on Surfactant Microstructure*

Figure 15 shows that the presence of Capstone and Glucocon in water has increased TMB solubility and the values are 0.12 and 0.18 wt.% respectively. We have observed the formation of multilayer vesicles, an increase in diameter of vesicles for Capstone (Figure 6), and one-dimensional growth of worm-like micelle of Glucocon (Table 5). Previous literature has shown that hydrocarbon surfactant diffuses to bulk along with the solubilized fuel molecules forming swollen micelle [39]. The data from this research indicates that micelle size increases due to the TMB solubility; however, the location of TMB molecules inside the micelle has not been verified. Further study would require locating the fuel molecules inside the micelle.

The solubility of fuel in surfactant solution will impact the interfacial properties. According to literature, once fuel molecules have higher surface activity, the effectiveness of the surfactants in keeping low IFT decreases, hence interfacial tension increases [40]. Interfacial tension (IFT) measurements (Figure 10) show higher IFT values for Capstone-TMB and Glucocon-TMB compared to Capstone-heptane and Glucocon-heptane respectively. The benzene ring increases the amphiphilicity or surface activity of TMB. Fuel concentration measurements (Figure 15) show that TMB has higher solubility in Capstone and Glucocon solution. The higher solubility of TMB in Capstone and Glucocon solution (Figure 15) causes surfactants to go away from the interface to the bulk and form structure at lower concentrations. Thus, increasing IFT value for Glucocon-TMB and Capstone-TMB, reduces surface excess (Figure 13) and decreases CMC (Figure 12). A comparable decrease in surface excess has also been reported for long chain alkylpolyglucoside surfactants in the presence of benzene ring fuels as second phase [39].

Figure 19 is the representation of the normalized value of surface excess. It is interesting to observe that when surface excess reduction is  $\sim 70\%$  or less microstructure seems to be changing in the presence of fuel. Microstructural and interfacial properties indicated that fuel solubility in surfactant solution is critical to fuel transport.

The fuel solubility in surfactant solution will have an impact on ignition time. From ignition tests we have observed that Capstone has higher ignition time irrespective of fuel type (Figure 18). Due to oleophobic and hydrophobic combination along with lowest surface tension, Capstone is the best performer. Capstone has longer ignition time compared to Glucocon for 25%TMB-75%heptane. The higher solubility of 25% TMB-75%heptane in Glucocon solution is the reason for shorter ignition time compared to Capstone solution. Hydrocarbon surfactant can solubilize 25%TMB-75%heptane fuel molecules more than fluorocarbon surfactant which follows the trend provided by Hinnant et al. [7]. Therefore, higher fuel solubility in surfactant solution causes shorter ignition time. The solubility of this fuel mixture in surfactant solutions increases due to the presence of TMB. In addition, TMB solubility in water increases due to Capstone and Glucocon. Therefore, due to higher solubility of TMB in surfactant solution observed changes in microstructure, interfacial properties, and shorter ignition time.

Higher vapor pressure decreases ignition time as well. Both octane and heptane have poor solubility in water (Table 8). None of the surfactants have increased

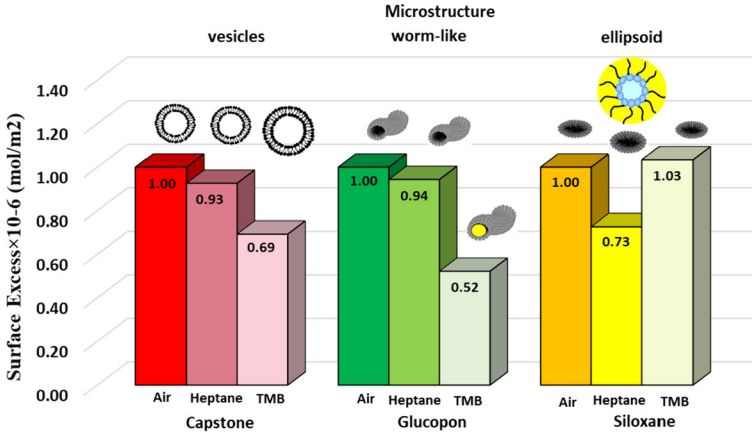


**Figure 19. Comparison of interfacial properties at air/solution and fuel/solution interface for Capstone, Glucopon, and siloxane to their microstructural properties.**

solubility of octane or heptane (Figure 14) in water. Nonetheless, the vapor pressure of heptane is higher than octane (Table 1) and higher vapor pressure decreases the ignition time in this instance. Hence, ignition time is shorter for heptane compared to octane (Figure 18). Although, the vapor pressure for heptane is 49 mm Hg higher than the vapor pressure of 25%TMB-75%heptane which is 37.9 mm Hg. However, ignition time for 25%TMB-75%heptane is shorter compared to heptane due to its higher solubility. Therefore, the poor solubility of heptane in Capstone and Glucopon solutions caused longer ignition time compared to 25%TMB-75%heptane. The fire extinguishment time has increased with increasing vapor pressure and fuel water solubility as shown by Briggs and Webb et al. [41]. In this work, we have shown that surfactant increases solubility of fuel in water. Then higher solubility of fuel decreases ignition time. It would be expected that a lower ignition time would correspond to a higher extinguishment time. Therefore, the trend for ignition test results is similar to the fire extinguishment tests by Biggs and Webb [41].

A low surface excess might be the reason for the poor performance of siloxane surfactant foam solution during ignition test. Figure 18 shows that siloxane foam solution has a very low ignition time for all the fuels tested. Heptane and TMB have poor solubility in siloxane surfactant solution (Figure 14). SANS result reveals that siloxane micelle size and shape do not have any effect of heptane or TMB (Table 6). However, surface excess for siloxane is smaller compared to Capstone and Glucopon (Figure 13). A lower surface excess means the number of surfactants at the interface is low which cannot provide enough resistance against fuel transport. A comparatively high expansion ratio (Table 9) and larger bubble size (Figure 17) have been observed for siloxane foam solution which means foams are comparatively dry, and a smaller number of surfactants are present throughout the foam solution. Therefore, lower surface excess and higher expansion

sion ratio might be the reason for poor performance of siloxane foam solution during ignition test.

Convection might have some effect on fuel transport. In foams, the solution is continuously draining down the foam due to gravity toward the fuel surface. The motion of the drained surfactant solution at the fuel surface induces convection at this interface. To explore the convection effect, stirring was introduced in the bottom phase of Capstone solution (Figure 3). Figure 16 shows that 25%TMB-75% heptane gets solubilized by Capstone solution when stirring was done in the bottom phase (Figure 3) which means convection might have an effect on surfactant foam solution draining. Glucocon solution can solubilize 25% TMB-heptane with and without stirring (Figure 16). Convection effect can be fuel and surfactant-type dependent, and further work is needed to fully understand this effect.

Vesicles formed by Capstone in the bulk might have some effect on the longer ignition time of Capstone compared with Glucocon. Vesicles might be more stable while capturing fuel [42] and not allowing fuel to be released in the gas phase compared to worm-like micelles of Glucocon. However, further studies will be required to confirm the impact of micelle shape on fuel transport.

## **5. Conclusion**

The analysis of fuel impact on single surfactants followed common trends. However, microstructural visualization of single surfactants provides direct evidence of the impact of fuel. Moreover, factors affecting microstructure and implication of this factor in ignition time.

Capstone forms vesicles at the nanoscale. The diameter and sometimes membrane layer thickness of the vesicles increase in the presence of TMB. Glucocon forms worm-like micelles, and one-dimensional growth occurs in the presence of TMB. Due to the higher solubility of TMB in Capstone and Glucocon solution, microstructural changes occur. Heptane does not impact Capstone and Glucocon microstructure. Due to the poor solubility of nonpolar fuel like heptane in Capstone and Glucocon solution microstructure is unaffected. Siloxane creates ellipsoidal micelles, and TMB or heptane does not impact the bulk microstructure rather siloxane forms reverse micelle in heptane. In addition, interfacial tension increases, surface excess, and CMC reduces due to the higher solubility of polar fuel like TMB in Capstone and Glucocon solution. Microstructural and interfacial properties show that fuel solubility in surfactant solution is an important factor during fuel transport.

Ignition time is shorter when microstructure and interfacial properties have shown an impact of fuel solubility. The higher solubility of 25%TMB-75%heptane in Capstone and Glucocon solution causes lower ignition time compared to heptane. However, heptane has a shorter ignition time than octane due to its higher vapor pressure. Moreover, siloxane has the lowest ignition time due to its low surface excess compared to Capstone and Glucocon solution. Therefore, ignition test results show that higher solubility of fuel in surfactant solution and higher vapor pressure, low surface excess impact ignition time. Overall, this study

highlights the significance of both surface excess and fuel solubility in surfactant solution as important properties when developing a novel surfactant.

## **Acknowledgements**

The authors would like to thank the SERDP for funding this effort. This research has used the resources of the Center for Nanophase Materials Sciences (CNMS) under CNMS user program and Spallation Neutron Source (SNS), which are DOE Office of Science User Facilities at Oak ridge national laboratory. The Cryo-TEM images were taken by scientist Dr. Alexis Williams from CNMS at ORNL. The SANS experiments were done by scientist Dr. Gergely Nagy from SNS facility at ORNL. We are thankful to Dr. Jong K. keum from CNMS at ORNL for helping us with the computational chemistry software Avogadro. The UV-Vis measurement has become possible using Virginia Tech's Materials Characterization Facility, which is supported by the Institute for Critical Technology and Applied Science, the Macromolecules Innovation Institute, and the Office of the Vice President for Research and Innovation. DLS measurements were possible due to shared facilities at the Nanoscale Characterization and Fabrication Laboratory, which is funded and managed by Virginia Tech's Institute for Critical Technology and Applied Science.

## **Funding**

This work was funded by Strategic Environmental Research and Development Program (Grant No. W912HQ22C0028).

## **Open Access**

This article is licensed under a Creative Commons Attribution 4.0 International License, which permits use, sharing, adaptation, distribution and reproduction in any medium or format, as long as you give appropriate credit to the original author(s) and the source, provide a link to the Creative Commons licence, and indicate if changes were made. The images or other third party material in this article are included in the article's Creative Commons licence, unless indicated otherwise in a credit line to the material. If material is not included in the article's Creative Commons licence and your intended use is not permitted by statutory regulation or exceeds the permitted use, you will need to obtain permission directly from the copyright holder. To view a copy of this licence, visit <http://creativecommons.org/licenses/by/4.0/>.

## SUPPLEMENTARY INFORMATION

The online version contains supplementary material available at <https://doi.org/10.1007/s10694-024-01577-x>.

## References

1. Baduel C, Mueller JF, Rotander A, Corfield J, Gomez-Ramos MJ (2017) Discovery of novel per- and polyfluoroalkyl substances (PFASs) at a fire fighting training ground and preliminary investigation of their fate and mobility. *Chemosphere* 185:1030–1038. [10.1016/j.chemosphere.2017.06.096](https://doi.org/10.1016/j.chemosphere.2017.06.096)
2. Place BJ, Field JA (2012) Identification of novel fluorochemicals in aqueous film-forming foams used by the US military. *Environ Sci Technol* 46(13):7120–7127. [10.1021/es301465n](https://doi.org/10.1021/es301465n)
3. Backe WJ, Day TC, Field JA (2013) Zwitterionic, cationic, and anionic fluorinated chemicals in aqueous film forming foam formulations and groundwater from U.S. military bases by nonaqueous large-volume injection HPLC-MS/MS. *Environ Sci Technol* 47(10):5226–5234. [10.1021/es3034999](https://doi.org/10.1021/es3034999)
4. Sheng Y, Jiang N, Lu S, Wang Q, Zhao Y, Liu X (2020) Study of environmental-friendly firefighting foam based on the mixture of hydrocarbon and silicone surfactants. *Fire Technol* 56(3):1059–1075
5. Ananth R, Hinnant KM, Giles SL, Farley JP, Snow AW (2020) Environmentally friendly surfactants for foams with low fuel permeability needed for effective pool fire suppression. Naval Research Lab Washington, Washington
6. <Characterizing trends between surfactant structure fuel transport through a foam layer.pdf>
7. Hinnant KM, Giles SL, Ananth R (2017) Measuring fuel transport through fluorocarbon and fluorine-free firefighting foams. *Fire Saf J* 91:653–661. [10.1016/j.fire-saf.2017.03.077](https://doi.org/10.1016/j.fire-saf.2017.03.077)
8. Hinnant KM, Giles SL, Snow AW, Farley JP, Fleming JW, Ananth R (2018) An analytically defined fire-suppressing foam formulation for evaluation of fluorosurfactant replacement. *J Surfactants Deterg* 21(5):711–722
9. Ananth R, Snow AW, Hinnant KM, Giles SL, Farley JP (2019) Synergisms between siloxane-polyoxyethylene and alkyl polyglycoside surfactants in foam stability and pool fire extinction. *Colloids Surf A* 579:123686
10. Hinnant K, Giles S, Smith E, Snow A, Ananth R (2020) Characterizing the role of fluorocarbon and hydrocarbon surfactants in firefighting-foam formulations for fire-suppression. *Fire Technol* 56(4):1413–1441
11. Williams B et al (2011) Extinguishment and Burnback tests of fluorinated and fluorine-free firefighting foams with and without film formation. In: *Suppression, detection, and signaling research and applications—a Technical Working Conference (SUPDET 2011)*
12. Snow AW, Giles S, Hinnant K, Farley J, Ananth R (2019) Fuel for firefighting foam evaluations: gasoline vs heptane. Naval Research Lab Washington, Washington
13. Ananth R, Snow A, Hinnant K, Giles S, Farley J (2021) Fluorine-free foams with oleophobic surfactants and additives for effective pool fire suppression. Naval Research Lab Washington, Washington
14. Jiang N, Sheng Y, Li C, Lu S (2018) Surface activity, foam properties and aggregation behavior of mixtures of short-chain fluorocarbon and hydrocarbon surfactants. *J Mol Liq* 268:249–255

15. Li X, Gao Y, Boott CE, Winnik MA, Manners I (2015) Non-covalent synthesis of supermicelles with complex architectures using spatially confined hydrogen-bonding interactions. *Nat Commun* 6(1):8127
16. Hill C et al (2018) Surface and bulk properties of surfactants used in fire-fighting. *J Colloid Interface Sci* 530:686–694
17. Langevin D (2020) On the rupture of thin films made from aqueous surfactant solutions. *Adv Coll Interface Sci* 275:102075
18. Stevenson P (2010) Inter-bubble gas diffusion in liquid foam. *Curr Opin Colloid Interface Sci* 15(5):374–381
19. Berret J-F, Herve P, Aguerre-Chariol O, Oberdisse J (2003) Colloidal complexes obtained from charged block copolymers and surfactants: A comparison between small-angle neutron scattering, Cryo-TEM, and simulations. *J Phys Chem B* 107(32):8111–8118
20. Fan Y, Wang Y (2019) Applications of small-angle X-ray scattering/small-angle neutron scattering and cryogenic transmission electron microscopy to understand self-assembly of surfactants. *Curr Opin Colloid Interface Sci* 42:1–16
21. National Center for Biotechnology Information (2024) PubChem Compound Summary for CID 8900, Heptane. Retrieved February 27, 2024 from <https://pubchem.ncbi.nlm.nih.gov/compound/Heptane>
22. National Center for Biotechnology Information (2024) PubChem Compound Summary for CID 356, Octane. Retrieved February 27, 2024 from <https://pubchem.ncbi.nlm.nih.gov/compound/Octane>
23. National Center for Biotechnology Information (2024) PubChem Compound Summary for CID 7247, 1,2,4-Trimethylbenzene. Retrieved February 27, 2024 from [https://pubchem.ncbi.nlm.nih.gov/compound/1\\_2\\_4-Trimethylbenzene](https://pubchem.ncbi.nlm.nih.gov/compound/1_2_4-Trimethylbenzene)
24. Snow AW, Giles S, Hinnant KM, Farley JP, Ananth R (2017) Quantification of fluorine content in AFFF concentrates. Naval Research Lab Washington, Washington
25. Eastoe J, Dalton J (2000) Dynamic surface tension and adsorption mechanisms of surfactants at the air–water interface. *Adv Coll Interface Sci* 85(2–3):103–144
26. Bastow T, Durnie WH, Jefferson A, Pang J (1997) Ultraviolet spectroscopy for the analysis of oil-in-water effluent using isopropanol as co-solvent. *Appl Spectrosc* 51(3):318–322
27. Israelachvili JN, Mitchell DJ, Ninham BW (1976) Theory of self-assembly of hydrocarbon amphiphiles into micelles and bilayers. *J Chem Soc* 72:1525–1568
28. Salim M, Minamikawa H, Sugimura A, Hashim R (2014) Amphiphilic designer nanocarriers for controlled release: from drug delivery to diagnostics. *MedChemComm* 5(11):1602–1618
29. Khalil RA, Al-hakam AZ (2014) Theoretical estimation of the critical packing parameter of amphiphilic self-assembled aggregates. *Appl Surf Sci* 318:85–89
30. Mosley GL, Yamanishi CD, Kamei DT (2013) Mathematical modeling of vesicle drug delivery systems 1: vesicle formation and stability along with drug loading and release. *J Lab Autom* 18(1):34–45
31. Hanwell MD, Curtis DE, Lonie DC, Vandermeersch T, Zurek E, Hutchison GR (2012) Avogadro: an advanced semantic chemical editor, visualization, and analysis platform. *J Cheminformatics* 4(1):1–17
32. Yu X et al (2021) Foaming behavior of fluorocarbon surfactant used in fire-fighting: the importance of viscosity and self-assembly structure. *J Mol Liq* 327:114811
33. Sato T et al (2006) Oil-induced structural change of wormlike micelles in sugar surfactant systems. *J Dispersion Sci Technol* 27(5):611–616

*Understanding the Impact of Fuel on Surfactant Microstructure*

34. Hinnant K (2021) Characterizing trends between surfactant structure, fuel transport through a foam layer, and foam fire extinction performance for firefighting foams containing novel environmentally-friendly surfactants. The George Washington University, Washington
35. Sulek MW, Wasilewski T (2008) Influence of critical micelle concentration (CMC) on tribological properties of aqueous solutions of alkyl polyglucosides. *Tribol Trans* 52 (1):12–20
36. Svitova T, Hill R, Smirnova Y, Stuermer A, Yakubov G (1998) Wetting and interfacial transitions in dilute solutions of trisiloxane surfactants. *Langmuir* 14(18):5023–5031
37. Hinnant KM et al (2020) Extinction performance summary of commercial fluorine-free firefighting foams over a 28 ft<sup>2</sup> pool fire detailed by MIL-PRF-24385. Naval Research Lab Washington, Washington
38. Koczko K, Racz G (1991) Foaming properties of surfactant solutions. *Colloids Surf* 56:59–82
39. Balzer D, Luders H (2000) Nonionic surfactants: alkyl polyglucosides. CRC Press, Boca Raton
40. Kutschmann E-M, Findenegg G, Nickel D, Von Rybinski W (1995) Interfacial tension of alkylglucosides in different APG/oil/water systems. *Colloid Polym Sci* 273:565–571
41. Briggs A, Webb J (1988) Gasoline fires and foams. *Fire Technol* 24:48–58
42. Gu D et al (2010) An aqueous emulsion route to synthesize mesoporous carbon vesicles and their nanocomposites. *Adv Mater* 22(7):833–837

**Publisher's Note** Springer Nature remains neutral with regard to jurisdictional claims in published maps and institutional affiliations.